Study of a Self-Contained Electro-Hydraulic Cylinder Drive

Daniel Hagen
Department of Engineering Sciences
University of Agder
Grimstad, Norway
daniel.hagen@uia.no

Damiano Padovani
Department of Engineering Sciences
University of Agder
Grimstad, Norway
damiano.padovani@uia.no

Morten K. Ebbesen
Department of Engineering Sciences
University of Agder
Grimstad, Norway
morten.k.ebbesen@uia.no

***Abstract*—Self-contained electro-hydraulic cylinders that can be powered just by an electrical wire will be popular in the coming years. Combining electrical-drives and hydraulic cylinders exploits some excellent properties of these two technologies and enables flexible implementation. To fully benefit from such a drive solution, there is the need to develop electro-hydraulic cylinders capable of operating independently as opposed to standard hydraulic systems that are connected to a central power supply. Therefore, this paper presents a numerical investigation of a self-contained electro-hydraulic cylinder with passive load-holding capability. The corresponding dynamic model is proposed and used to predict the system behavior with a view to future implementation. The simulations show the proposed drive guarantees proper functioning in four-quadrant operations.**

***Index Terms*—compact electro-hydraulic cylinders, valve-less systems, electric-drives, load-holding**

I. Introduction

During the last years, electro-mechanical drives are increasingly replacing standard valve-controlled hydraulic actuators due to the easy installation on the machine and the higher energy efficiency [1]. These electro-mechanical solutions are unsuitable in several applications such as primary aircraft flight control or offshore oil drilling mainly due to the limited reliability [2]. For this reason, there is an ongoing interest in developing self-contained electro-hydraulic cylinders (SCCs) since they represent a valid alternative to electro-mechanical systems. SCCs are compact and self-sufficient drives connected to an electrical power supply that enable plug-and-play installation (Fig. 1). A limited number of commercial SCCs have been introduced to the market mainly using single-rod cylinders [3]. Employing a valve-less architecture to control the hydraulic actuator is popular in many applications since higher energy efficiency is possible. For instance, a displacement-controlled excavator showed a 40% efficiency improvement in a truck loading cycle when compared to a state-of-the-art load-sensing machine [4]. Research focus related to SCCs is primarily on cost efficiency and low power applications, i.e. below 5 kW [5]. For instance, Michel et al. derived specific conclusions about the best approach for SCCs without passive load-holding functions [6]. This means there is need for more generic SCCs capable of delivering higher power and providing features such as passive load-holding. Countless applications will benefit from such a drive solution. A few examples are gripper arms for offshore pipe handling machines [2], hydraulic presses, trailer lifts, marine jack plates, scissors tables, positioning systems for solar panels, Stewart platforms, single-boom cranes, etc. Thus, this paper takes advantage of a comprehensive literature study on electro-hydraulic architectures to discuss a concept for a self-contained cylinder. The target is on the evaluation of an electro-hydraulic self-contained single-rod cylinder in closed-circuit configuration with sealed tank suitable for power levels above 5 kW. The mathematical model of the proposed system is presented together with a numerical investigation intended to evaluate the performance in view of a future implementation.

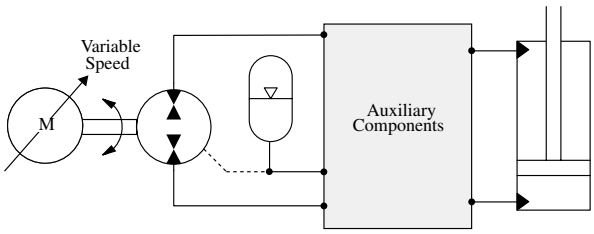

Fig. 1: Standard system architecture for self-contained electro-hydraulic cylinders (simplified schematic).

II. Literature Survey

The majority of valve-less systems in closed-circuit configuration makes use of the following approaches to control the motion of linear actuators.

1) Systems with a variable-displacement pump driven at fixed speed. The amount of flow directed to the actuator is controlled by the pump displacement setting while the flow direction is changed by adjusting the swash-plate overcenter. Figure 2 shows the system in closed-circuit configuration presented in [7]. This control approach is mainly used for multi-actuator construction machines, e.g. [4], since a dedicated pressure source is needed to adjust the unit displacements.

2) Systems with a variable-speed electric motor driving the fixed-displacement pump. The actuator motion is controlled

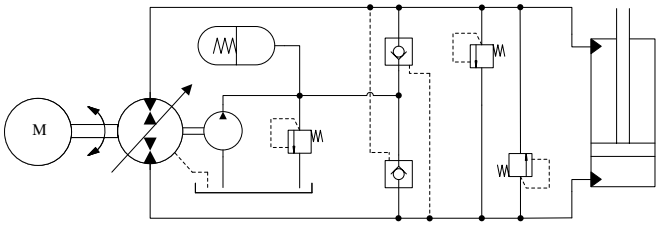

Fig. 2: Displacement-controlled pump driving a single-rod cylinder according to the architecture proposed in [7].

by adjusting both speed and direction of the motor rotation [6], [8], [9], [10], (Fig. 3). The electric motor can either be an asynchronous machine [11] or a synchronous machine [8].

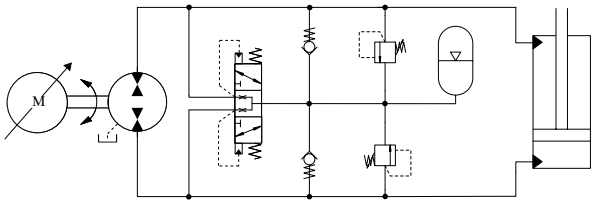

Fig. 3: Speed-controlled pump driving the cylinder according to the architecture proposed in [10].

3) Systems with a combined control method. The variable-speed prime mover drives the variable-displacement servo-pump meaning that both components are actively controlling the actuator motion [12].

Only layouts with a variable-speed electric motor and a fixed-displacement pump have been consistently used for SCCs in the past. This minimizes the number of control elements and the number of hydraulic components, i.e. the additional pressure source of the variable-displacement pump is not needed. Concerning the actuator type, double-rod cylinders are almost exclusively used in aircraft flight controls [13], [14], [15], [16] and [17]. The double-rod configuration increases the installation space while the symmetrical piston areas reduce the maximum available force with the same maximum pressure. Consequently, single-rod cylinders are the most popular actuators for at least 80% of electro-hydraulic drives [18]. Balancing the differential flow due to the asymmetric areas is necessary when the closed-circuit configuration is implemented. Multiple flow compensation methods were proposed in the past mainly involving pilot operated check valves (Fig. 2), flushing valves (Fig. 3), or electrically operated on/off valves [19]. Some issues related to instability and uncontrolled pressure oscillations were mentioned [10] and [20]. However, this is the case under high dynamic excitations of the system [3], i.e. an operating condition that might be representative for low-power applications. Other approaches have also been explored such as using hydraulic transformers, tandem pumps, 3-port axial-piston pumps, asymmetric gear pumps, or two pumps connected to each actuator port (Fig. 4). Table I provides a synthesis of these options.

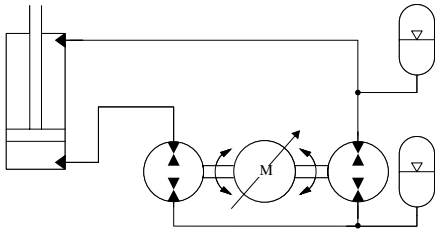

Fig. 4: Simplified architecture according to [8] of a SCC with two gear units that balance the differential cylinder flow.

Moreover, very few researches addressed the passive load-holding capability of SSCs. This feature is intended to maintain a fixed piston position without delivering power to the system. A first solution is a commercialized system [21] that has been patented in 2008 [22]. Pilot operated check valves are installed between the pump and the actuator while each opening pilot is sensing the pressure of the opposite pump side, see Fig. 5. A similar approach is also addressed in [23] and [24]. Alternative load-holding systems were presented in [9] and [25]. Both solutions make use of counterbalance valves that are operated differently. Some of these load-holding systems are also equipped with manual pressure release valves that can be used in case of failure to manually modify the actuator position.

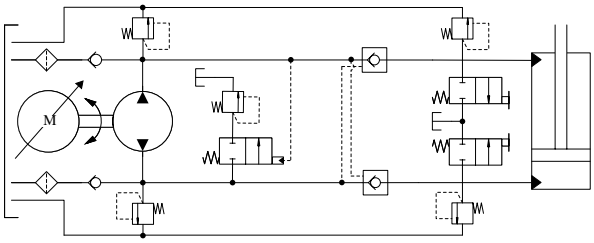

Fig. 5: Closed-circuit configuration with passive load-holding according to [21].

TABLE I: Differential flow compensation methods

Method:	**Reference:**
Hydraulic transformers	[26], [27], [28]
Pilot operated check valves	[7], [24], [29], [30], [31]
Shuttle valve	[6], [32], [33]
Tandem pumps	[34]
3-port asymmetric piston pump	[35], [36], [37], [38]
Asymmetric gear pump	[39]
Two pumps with equal displacement	[40]
Two pumps with different displacement	[6], [41], [42]
Two single rod cylinders in parallel	[43]

Table II summarizes the architectures of the SCCs addressed in this survey. Details about the possibility of performing four quadrant (4Q) operations are listed as well as the passive load-holding (PLH) capability.

In conclusion, the idea behind electro-hydraulic self-contained cylinders is combining the advantages of standard

hydraulic actuators such as reliability, and high power-to-weight ratio, with the benefits of electro-mechanical drives such as energy efficiency, minimal maintenance, and easy plug-and-play commissioning. Additional requirements such as compactness, robustness, and reduced costs are also of interest due to their relevance in both industrial and mobile applications [3] and [39].

TABLE II: List of considered SCC concepts

SCCs:	4Q:	PLH:	Reference:
Double gear pump	YES	NO	[6]
Direct driven hydraulic drive	YES	NO	[8]
Differential gear pump	NO	NO	[39], [44]
Inverse shuttle valve	YES	NO	[3], [6], [45]
Compact electro-hydraulic actuator	NO	YES	[9], [25]
Pump controlled single rod actuator	YES	NO	[10], [46]
Compact electro-hydraulic actuator	NO	YES	[21], [22]

III. System Architecture

The target of this research is to study a self-contained cylinder that operates in four quadrants, includes passive load-holding devices, and can deal with power levels above 5 kW. According to the literature survey presented in the previous section, published solutions that meet all these requirements are not available. Several systems represent a partial fit (Tab. II). Therefore, some features coming from them were combined accordingly to generate the architecture depicted in Fig. 6.

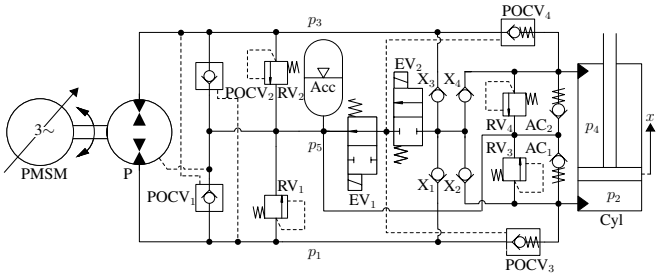

Fig. 6: Schematic of the SCC under investigation.

The combination of a variable-speed servo-motor (PMSM) and a fixed-displacement hydraulic pump was chosen to drive a single-rod cylinder arranged in closed-circuit configuration. Two pilot operated check valves ($\text{POCV}_{1,2}$) balance the differential cylinder flow as in the system discussed before [7]. Their low-pressure ports are connected to the accumulator (Acc) that represents the sealed tank of the SCC. The remaining pilot operated check valves ($\text{POCV}_{3,4}$) take care of the passive load-holding as in [21] and [23]. The opening pilot pressure is selected as the highest system pressure by some check valves ($\text{X}_{1,2,3,4}$) to deal properly with aided loads (i.e. when the load is acting in the same direction as the motion). This solution has been inspired by [47] where a 3/2 valve controls the opening pilot of the load-holding POCVs by using an external pressure signal always high enough. The passive load-holding is enabled or disabled by two electrically operated on/off valves (EV). When actuator motion is desired, the EVs are energized resulting in the opening pilot pressure equal to the highest system pressure. Conversely, when the EVs are not energized the pilot pressure is equal to the accumulator pressure that maintains $\text{POCV}_{3,4}$ closed. Pressure relief valves ($\text{RV}_{1,2,3,4}$) are installed on the pump ports and on the actuator ports to avoid overpressurizations during normal functioning and load-holding, respectively. An anti-cavitation valve (AC) is connected to each actuator side. Finally, a manually operated valve intended to release the actuator in case of electric failure is not showed in the schematic but can be easily included in the real system.

Figure 7 shows the functioning of the system under investigation depending on the operating condition. Low-pressure sides (LP) and high-pressure sides (HP) are highlighted in all four quadrants as well as the direction of the flows. The two on/off valves are always energized to disable the load-holding capability.

The size of the components has been chosen from catalogues available on the market according to a conventional static sizing that guarantees maximum piston speed of 150 $\frac{mm}{s}$ and maximum output force of 40 kN. This target is met assuming system pressure up to 200 bar in combination with a cylinder characterized by dimensions 65x35x500 mm. The resulting axial-piston pump has displacement of 10 $\frac{cm^3}{rev}$ since the selected servo-motor can run up to 4200 $\frac{rev}{min}$. This unit is a permanent magnet synchronous machine. Lastly, accumulator has a volume of 3.5 $liters$ whereas the load-holding valves have area ratio of 1:3 and cracking pressure of 5 bar.

IV. System Modeling

The hydraulics has been modeled using a well-established approach successfully tested in the past, e.g. by Rahmfeld [19]. The effective magnitudes of the pump are evaluated using flow and torque losses ($Q_S \geq 0$ and $T_S \geq 0$, respectively) measured from steady-state experimental data [48] with a reference unit. The same losses have been assumed for all quadrants and scaled to the desired pump displacement according to (1) and (2). The shaft speed as been scaled via (3).

$$Q_S = \lambda^2 \cdot Q_{S,ref} \tag{1}$$

$$Q_T = \lambda^3 \cdot Q_{T,ref} \tag{2}$$

$$n = \lambda^3 \cdot n_{ref} \tag{3}$$

The scaling factor λ is computed in (4) as function of the pump displacement D_P used in the simulation.

$$\lambda = \sqrt[3]{\frac{D_P}{D_{P,ref}}} \tag{4}$$

The effective unit flow rate is evaluated in (5) according to the machine operation, i.e. pumping or motoring mode. The flow losses are completely attributed to internal losses.

$$Q_P = \begin{cases} (|D_P \cdot n| - Q_S) \cdot sign(n), & \text{if pumping,} \\ (|D_P \cdot n| + Q_S) \cdot sign(n), & \text{otherwise.} \end{cases} \tag{5}$$

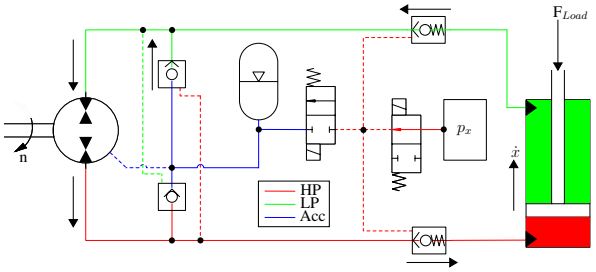

(a) Out-stroke, resistant load.

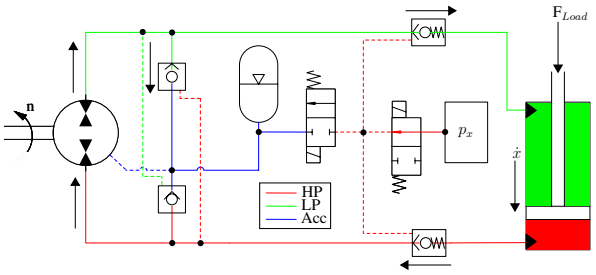

(b) In-stroke, aided load.

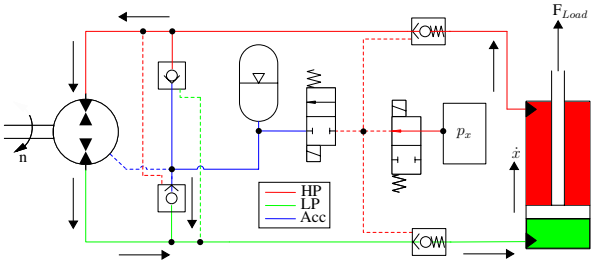

(c) Out-stroke, aided load.

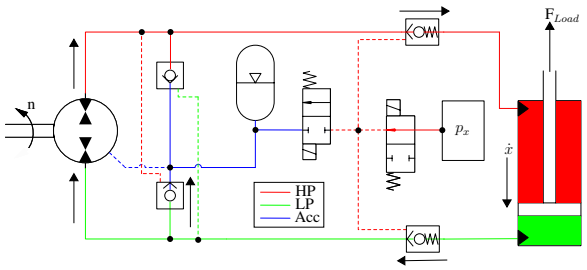

(d) In-stroke, resistant load.

Fig. 7: Four quadrant operations for the considered SCC (simplified schematics).

Equation (6) provides the effective shaft torque T_e.

$$T_e = \left(D_P \cdot \frac{\Delta p}{2\pi} + T_S\right) \cdot sign(n) \tag{6}$$

The mechanical powers measured at the unit shaft P_{Unit} and at the actuator rod P_{Cyl} are defined in (7) and (8).

$$P_{Unit} = T_e \cdot n \cdot sign(n) \tag{7}$$

$$P_{Cyl} = F_{Load} \cdot \dot{x} \tag{8}$$

Evaluating the pressures in the different sections of the system is crucial, and they are labeled in Fig. 6. The pressure build-up equation (9) that involves the fluid bulk modulus β, the volume of the hydraulic capacitance V and the flow balance has been used.

$$\dot{p} = \frac{\beta}{V} \cdot \sum_i Q_i \tag{9}$$

The pressure gradients related to every hydraulic capacitance are shown in details in (10), (11), (12), (13) and (14).

$$\dot{p_1} = \frac{\beta}{V_1} \cdot (Q_{POCV_1} + Q_P - Q_{POCV_3} - Q_{RV_1}) \tag{10}$$

$$\dot{p_2} = \frac{\beta}{V_2} \cdot (Q_{POCV_3} + Q_{AC_1} - \dot{x} \cdot A_A - Q_{RV_3}) \tag{11}$$

$$\dot{p_3} = \frac{\beta}{V_3} \cdot (Q_{POCV_2} - Q_{POCV_4} - Q_P - Q_{RV_2}) \tag{12}$$

$$\dot{p_4} = \frac{\beta}{V_4} \cdot (Q_{POCV_4} + Q_{AC_2} + \dot{x} \cdot A_B - Q_{RV_4}) \tag{13}$$

$$\dot{p_5} = \frac{\beta}{V_5} \cdot (Q_{RV_{1,2,3,4}} - Q_{POCV_{1,2}} - Q_{AC_{1,2}}) \tag{14}$$

Constant volumes V_0 have been assumed for the transmission lines V_1 and V_3. The definitions of the volumes V_2 and V_3 are shown in (15) and (16) respectively. The influence of the hydro-pneumatic accumulator is showed in (17), where γ is the polytrophic coefficient, $V_{0,Acc}$ the accumulator volume, and $p_{0,Acc}$ the pre-charge pressure.

$$V_2 = V_{0,2} + A_A \cdot x \tag{15}$$

$$V_4 = V_{0,4} + A_B \cdot (x_{max} - x) \tag{16}$$

$$V_5 = V_{0,5} + \left(\beta \cdot \frac{V_{0,Acc}}{\gamma} \cdot \frac{p_{0,Acc}{}^{\frac{1}{\gamma}}}{p_5^{\frac{\gamma+1}{\gamma}}}\right) \tag{17}$$

The flow rates of the anti-cavitation valves ($i = \mathrm{AC}_{1-2}$) and of the pressure relief valves ($i = \mathrm{RV}_{1-4}$) are defined in (18). The characteristic valve flow gain K_i is introduced as well as the inlet pressure p_{In}, the outlet pressure p_{Out}, and the cracking pressure p_{Cr}.

$$Q_i = \begin{cases} K_i \cdot (p_{In} - p_{Out} - p_{Cr}), & \text{if } (p_{In} - p_{Out}) \geq p_{Cr}, \\ 0, & \text{otherwise.} \end{cases} \tag{18}$$

The flow rate through the pilot-operated check valves ($i = \mathrm{POCV}_{1-4}$) is found with the orifice equation (19). The different terms are the discharge coefficient C_d, the seat diameter d, the lift of the poppet y, the pressure differential across the valve Δp and the fluid density ρ.

$$Q_i = C_d \cdot (\pi \cdot d_i \cdot y_i) \cdot sign\,(\Delta p_i) \cdot \sqrt{\frac{2}{\rho} \cdot |\Delta p_i|} \tag{19}$$

The lift results from the force equilibrium of the poppet where the poppet dynamics have been neglected. The pilot pressure p_x, the area of the poppet seat A_{Seat}, the area of the pilot stage A_x, the pre-load force of the spring $F_{S,0}$, and the spring stiffness k_S are involved. Two operating modes are emphasized: normal flow (20) when the pilot stage is separated

from the poppet (i.e. $p_{In} > p_x$) and reverse flow direction (21) if the pilot stage is in contact with the poppet (i.e. $p_{In} < p_x$).

$$y_i = \frac{1}{k_S} \cdot (\Delta p_i \cdot A_{Seat} - F_{S,0}) \tag{20}$$

$$y_i = \frac{1}{k_S} \cdot ((p_x - p_{In}) \cdot A_x + \Delta p_i \cdot A_{Seat} - F_{S,0}) \tag{21}$$

The governing equation for the actuator motion is pointed out in (22) from the Newton's second law. A simplified scenario characterized by a horizontal sliding mass m_{Eq} loaded by an external force F_{Load} is accounted.

$$\ddot{x} = \frac{1}{m_{Eq}} \cdot (p_2 \cdot A_A - p_4 \cdot A_B - F_{Fric} - F_{Load}) \tag{22}$$

The actuator pressures and areas (piston-side area A_A and rod-side area A_B) describe the force coming from the hydraulics while the actuator friction F_{Fric} is given in (23) according to the Stribeck model. The different coefficients account the viscous friction coefficient f_V, the Coulomb friction F_C, and the static friction coefficient f_S.

$$F_{fric} = \dot{x} \cdot f_V + sign(\dot{x}) \cdot \left(F_C + f_S \cdot e^{-\frac{|\dot{x}|}{\tau_S}}\right) \tag{23}$$

The pressure losses in the transmission lines have been neglected due to the compact configuration of the drive. The valves used to enable/disable the load-holding capability have been simulated as an equivalent logic function. Finally, the dynamics of the electric motor have been simulated using a second-order transfer function from commanded to simulated speed. Due to the fast response of the machine, this simplified approach is sufficient at this stage of the investigation.

V. Simulation Results

Understanding if the proposed SCC is a feasible approach to meet the aforementioned requirements represents the target of the following simulations. Operations in four quadrants are tested by varying the direction of the external load accordingly. The controller implemented in MATLAB-Simulink takes care of generating the commanded motor speed in order to track the desired actuator position. The logic emerges from Fig. 8. The command directed to the on/off valves (not shown in the block diagram) is activated when non-zero actuator velocity is wanted.

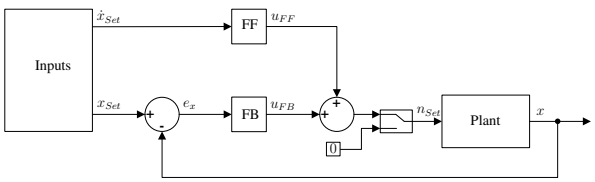

Fig. 8: The control logic for the proposed SCC.

If actuator motion is not desired, the switch logic sets the commanded motor speed to zero. Contrariwise, the motor speed is defined as follows. The feedforward term (FF) estimates the necessary motor speed depending if the HP is on the piston-side or on the rod-side (24).

$$u_{FF} = \begin{cases} \dot{x}_{Set} \cdot \left(\frac{A_A}{D_P}\right), & \text{if HP} \rightarrow \text{piston-side,} \\ \dot{x}_{Set} \cdot \left(\frac{A_B}{D_P}\right), & \text{otherwise.} \end{cases} \tag{24}$$

The feedback element (FB), originated by a constant gain K_P acting on the position error e_x, corrects the prediction of the feedforward element. The resulting speed command n_{Set} is propagated to the plant according to (25).

$$n_{Set} = e_x \cdot K_P + u_{FF} \tag{25}$$

Figure 9 depicts the actuator position in combination with the position error and the external load acting on the actuator. The results show good agreement between commanded and simulated position. This is the case for system operations in all four quadrants (OUT $\rightarrow$ cylinder out-stroke, IN $\rightarrow$ cylinder in-stroke, R $\rightarrow$ resistant load, and A $\rightarrow$ aided load).

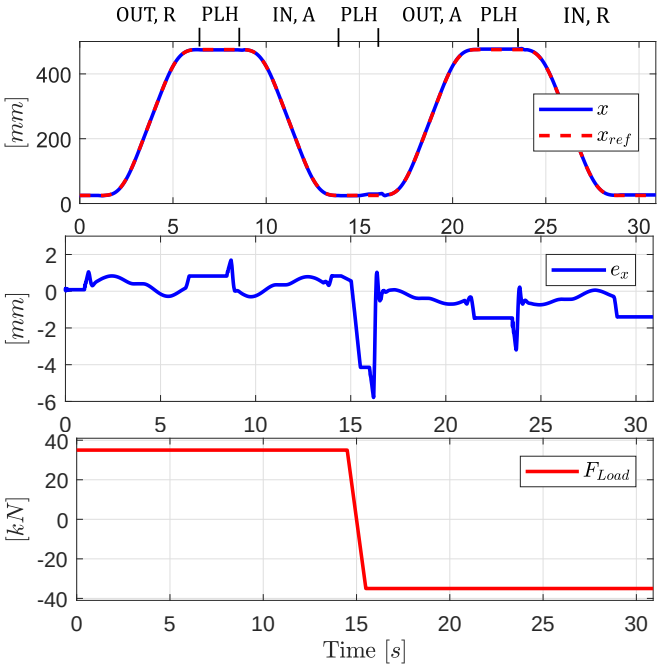

Fig. 9: Simulation cycle: piston position, position error, and load force.

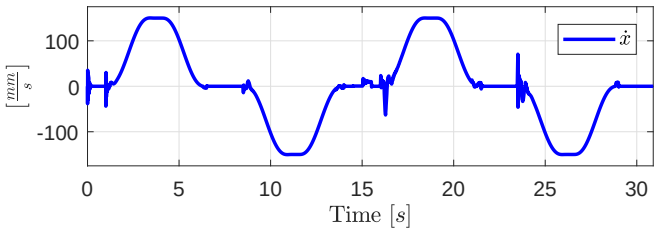

Fig. 10: Simulated actuator velocity.

The reference position has been generated to achieve the maximum piston velocity, i.e. 150 $\frac{mm}{s}$. Figure 10 proves

the system sizing is satisfactory. The control effort, i.e. the commanded motor speed, is presented in Fig. 11. The speed variation is generally very smooth and well within the upper limit of the electric machine. A few reduced spikes are induced by the zero-velocity switch logic that kicks in. The system pressures are visible in Fig. 12. They behave as expected, especially the accumulator pressure that is characterized by limited variations. Figure 13 highlights the poppet position of the load-holding pilot operated check valves $\text{POCV}_{3,4}$. The electric signal directed to the EVs to supervise the load-holding capability is included as well. The POCVs do not introduce unpleasant oscillations during motion. Most importantly, they maintain the piston position (Fig. 9) when the electric motor is not operating.

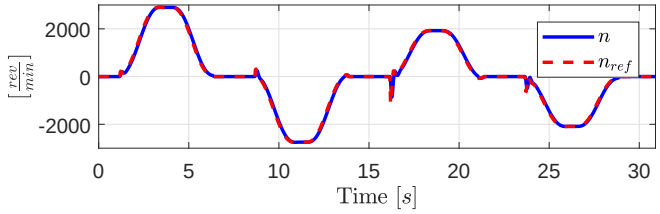

Fig. 11: Commanded and simulated motor speed.

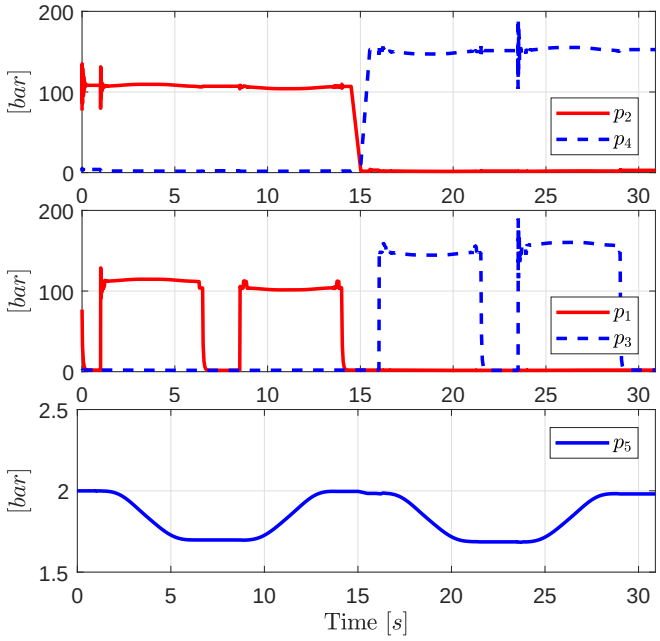

Fig. 12: System pressures: actuator, pump, and accumulator.

Figure 14 illustrates the mechanical power measured both at the unit shaft and at the actuator rod. According to the sign convention, positive values mean the power flow is from the hydraulic unit to the actuator and vice versa for negative values. The power levels presented are relatively low because they refer to a compact system meant for laboratory testing. Nevertheless, this system architecture can successfully deal with much higher power levels if the size of the components

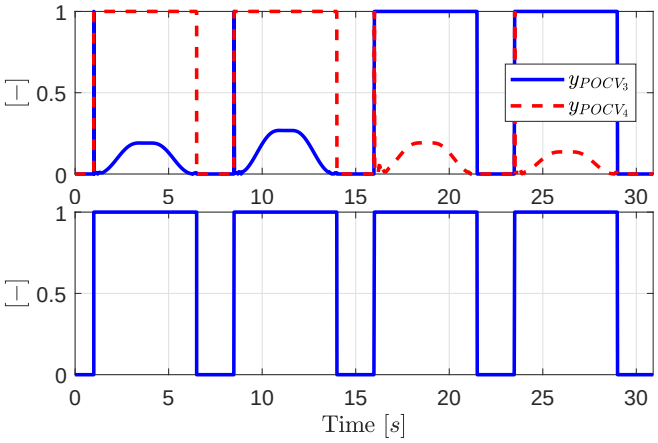

Fig. 13: Load-holding: poppet lift, and EV signal.

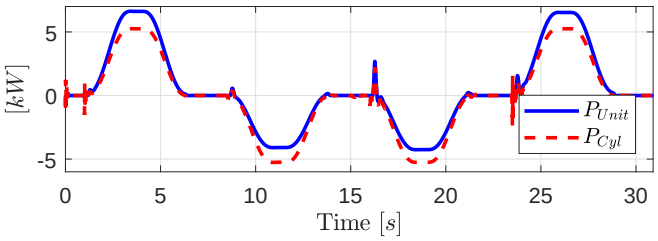

Fig. 14: Actuator and pump power.

is modified accordingly. Finally, these power trends provide some preliminary indications about the efficiency of the hydraulic sub-system. When the actuator is driven, this efficiency is about 80%.

VI. Conclusion

This paper discussed in first place a detailed literature review about electro-hydraulic self-contained cylinders characterized by being a sealed system. The survey pointed out a missing solution to drive SCCs that comprise passive load-holding devices, operate in four quadrants, and are suitable for power levels above 5 kW. Hence, a specific concept was presented and modeled. The numerical simulations showed that the system behaves properly in four quadrant operations and can hold the external load passively. Plans for future investigations include both the design of a more advanced control algorithm and the implementation of this SCC on a real test-bed.

Acknowledgment

The research presented in this paper has received funding from the Norwegian Research Council, SFI Offshore Mechatronics, project number 237896.

References

[1] E. Jalayeri, A. Imam, Z. Tomas, and N. Sepehri, "A throttle-less single-rod hydraulic cylinder positioning system: Design and experimental evaluation," *Advances in Mechanical Engineering*, vol. 7, no. 5, pp. 1–14, 2015.

[2] D. Hagen, W. Pawlus, M. K. Ebbesen, and T. O. Andersen, "Feasibility Study of Electromechanical Cylinder Drivetrain for Offshore Mechatronic Systems," *Modeling, Identification and Control*, vol. 38, no. 2, pp. 59–77, 2017.

[3] S. Michel and J. Weber, "Electrohydraulic Compact-drives for Low Power Applications considering Energy-efficiency and High Inertial Loads," *The 7th FPNI PhD Symposium on Fluid Power*, pp. 1–18, 2012.

[4] J. Zimmerman, E. Busquets, and M. Ivantysynova, "40% Fuel Savings by Displacement Control Leads to Lower Working Temperatures – A Simulation Study and Measurements," in *52nd National Conference on Fluid Power*, 2011.

[5] J. Weber, B. Beck, E. Fischer, G. Kolks, J. Lübbert, S. Michel, M. Schneider, R. Ivantysyn, L. Shabi, M. Kunkis, A. Sitte, H. Lohse, and J. Weber, "Novel System Architectures by Individual Drives," in *10th International Fluid Power Conference*, 2016, pp. 29–62.

[6] S. Michel and J. Weber, "Energy-efficient electrohydraulic companct drives for low power applications," *ASME/BATH 2012 Symposium on Fluid Power and Motion Control*, pp. 93–107, 2012.

[7] R. Rahmfeld and M. Ivantysynova, "Energy saving hydraulic actuators for mobile machines," in *1st Bratislavian Fluid Power Symposium*, 1998, pp. 177–186.

[8] T. a. Minav, P. Sainio, and M. Pietola, "Direct Driven Hydraulic Drive Without Conventional Oil Tank," in *ASME/BATH 2014 Symposium on Fluid Power and Motion Control*, no. September, 2014, pp. 1–6.

[9] G. Altare and A. Vacca, "A design solution for efficient and compact electro-hydraulic actuators," in *Procedia Engineering*, vol. 106. Elsevier Ltd, 2015, pp. 8–16.

[10] H. Çalışkan, T. Balkan, and B. E. Platin, "A Complete Analysis for Pump Controlled Single Rod Actuators," in *10th International Fluid Power Conference*, 2016, pp. 119–132.

[11] S. H. Cho and R. Burton, "Position control of high performance hydrostatic actuation system using a simple adaptive control (SAC) method," *Mechatronics*, vol. 21, pp. 109–115, 2011.

[12] J. Willkomm, M. Wahler, and J. Weber, "Potentials of Speed and Displacement Variable Pumps in Hydraulic Applications," in *10th International Fluid Power Conference*, 2016, pp. 379–391.

[13] S. Croke and J. Herrenschmidt, "More Electric Initiative Power-By-Wire Actuation Alternatives," in *Proceedings of National Aerospace and Electronics Conference (NAECON'94)*, 1994, pp. 1338–1346.

[14] S. Frischemeier, "Electrohydrostatic Actuators for Aircraft Primary Flight Control - Types, Modelling and Evaluation," in *5th Scandinavian International Conference on Fluid Power*, 1997, pp. 1–16.

[15] B. Kazmeier, "Energieverbrauchsoptimierte Regelung eines elektrohydraulischen Linearantriebs kleiner Leistung mit drehzahlgeregeltem Elektromotor und Verstellpumpe," Ph.D. dissertation, TU Hamburg-Harburg, 1998.

[16] L. Jun, F. Yongling, Z. Guiying, G. Bo, and M. Jiming, "Research on fast response and high accuracy control of an airborne brushless DC motor," in *Proceedings of the 2004 IEEE International Conference on Robotics and Biomimetics*, 2004, pp. 807–810.

[17] D. van den Bossche, "The A380 Flight Control Electrohydrostatic Actuators, Achievements and Lessons Learnt," in *25th International Congress of the Aeronautical Sciences*, 2006, pp. 1–8.

[18] Z. Quan, L. Quan, and J. Zhang, "Review of energy efficient direct pump controlled cylinder electro-hydraulic technology," *Renewable and Sustainable Energy Reviews*, vol. 35, pp. 336–346, 2014.

[19] R. Rahmfeld, "Development and Control of Energy Saving Hydraulic Servo Drives for Mobile Systems," Ph.D. dissertation, TU Hamburg-Harburg, 2002.

[20] C. Williamson and M. Ivantysynova, "Stability and Motion Control of Inertial Loads with Displacement Controlled Hydraulic Actuators," in *6th FPNI - PhD Symposium*, West Lafayette, 2010, pp. 499–514.

[21] Parker Hannifi, "Compact EHA - Electro-Hydraulic Actuators for high power density applications." [Online]. Available: https://goo.gl/t2FMw2

[22] T. Sweeney, P. T. Kubinski, and D. J. Anderson, "Electro-hydraulic actuator mounting, Patent US 8161742 B2," 2008.

[23] Bosch Rexroth, "Advantages of electrification and digitalization technology for hydraulics." [Online]. Available: https://goo.gl/4G6Jxn

[24] G. Li, H. Wang, X. Huang, and H. Yang, "Research on the Control Scheme of Direct Drive Electro-hydraulic Position Servo System," in *Proceedings of 2011 International Conference on Electronic and Mechanical Engineering and Information Technology, EMEIT 2011*, vol. 6, 2011, pp. 3221–3224.

[25] G. Altare, A. Vacca, and C. Richter, "A Novel Pump Design for an Efficient and Compact Electro-Hydraulic Actuator," in *IEEE Aerospace Conference*, 2014, pp. 1–8.

[26] J. Lodewyks, "Differenzialzyliner im geschlossenen hydrostatischen Getriebe," *O + P "Ölhydraulik und Pneumatik" 34 Nr.5*, pp. 394–401, 1993.

[27] ——, "Der Differentialzylinder im geschlossenen hydrostatischen Kreislauf," Ph.D. dissertation, RWTH Aachen, 1994.

[28] G. Vael, P. Achten, and J. Potma, "Cylinder Control With Floating Cup Hydraulic Transformer," pp. 175–190, 2003.

[29] Vickers Inc., "Electrohydraulic system and apparatus with bidirectional electric-motor hydraulic-pump unit, Patent WO 1998011358 A1," 1998.

[30] J.-m. Zheng, S.-d. Zhao, and S.-g. Wei, "Application of self-tuning fuzzy PID controller for a SRM direct drive volume control hydraulic press," *Control Engineering Practice*, vol. 17, no. 12, pp. 1398–1404, 2009.

[31] S. G. Wei, S. D. Zhao, J. M. Zheng, and Y. Zhang, "Self-tuning deadzone compensation fuzzy logic controller for a switched-reluctance-motor direct-drive hydraulic press," *Proceedings of the Institution of Mechanical Engineers, Part I: Journal of Systems and Control Engineering*, vol. 223, no. 5, pp. 647–656, 2009.

[32] A. J. Hewett, "Hydraulic circuit flow control, Patent US 5329767 A," 1994.

[33] L. Wang, W. J. Book, and J. D. Huggins, "A Hydraulic Circuit for Single Rod Cylinders," *Journal of Dynamic Systems, Measurement, and Control*, vol. 134, no. 1, pp. 1–11, 2012.

[34] K. Cleasby and A. Plummer, "A novel high efficiency electrohydrostatic flight simulator motion system," *ASME/BATH 2008 Symposium on Fluid Power and Motion Control*, pp. 437–449, 2008.

[35] R. L. Kenyon, D. Scanderbeg, M. E. Nolan, and W. D. Wilkerson, "Electro-hydraulic actuator, Patent EP0395420 A2," 1990.

[36] L. Quan, "Current State, Problems and the Innovative Solution of Electro-hydraulic Technology of Pump Controlled Cylinder," *Chinese Journal of Mechanical Engineering*, vol. 44, no. 11, pp. 87–92, 2008.

[37] X. Zhang, L. Quan, Y. Yang, C. Wang, and L. Yao, "Output Characteristics of a Series Three-port Axial Piston Pump," *Chinese Journal Of Mechanical Engineering*, vol. 25, no. 3, 2012.

[38] J. Huang, L. Quan, and X. Zhang, "Development of a dual-acting axial piston pump for displacement-controlled system," *Proceedings of the Institution of Mechanical Engineers, Part B: Journal of Engineering Manufacture*, vol. 228, no. 4, pp. 606–616, 2014.

[39] B. Brahmer, "CLDP - Hybrid Drive using Servo Pump in Closed Loop," in *Proceedings of 8th International Fluid Power Conference*, 2012, pp. 93–102.

[40] S. Helduser, "Electric-hydrostatic drive—an innovative energy-saving power and motion control system," *Proceedings of the Institution of Mechanical Engineers, Part I: Journal of Systems and Control Engineering*, vol. 213, no. 5, pp. 427–437, 1999.

[41] H. C. Pedersen, L. Schmidt, T. O. Andersen, and M. H. Brask, "Investigation of New Servo Drive Concept Utilizing Two Fixed Displacement Units," *JFPS International Journal of Fluid Power System*, vol. 8, no. 1, pp. 1–9, 2014.

[42] T. Minav, C. Bonato, P. Sainio, and M. Pietola, "Direct Driven Hydraulic Drive," in *The 9th International Fluid Power Conference*, 2014.

[43] T. Wiens and D. Bitner, "An Efficient, High Performance And Low-Cost Energy Recovering Hydrostatic Linear Actuator Concept," in *ASME/BATH 2016 Symposium on Fluid Power and Motion Control*, 2016, pp. 1–10.

[44] VOITH, "Servo Drive CLDP - Technical Data Sheet." [Online]. Available: https://goo.gl/mAHm4X

[45] S. Michel and J. Weber, "Prediction of the thermo-energetic behaviour of an electrohydraulic compact drive," in *10th International Fluid Power Conference*, 2016, pp. 219–234.

[46] H. Çalışkan, T. Balkan, and B. E. Platin, "A Complete Analysis and a Novel Solution for Instability in Pump Controlled Asymmetric Actuators," *Journal of Dynamic Systems, Measurement, and Control*, vol. 137, no. 9, pp. 1–14, 2015.

[47] T. I. Hwang, "Hydraulic circuit with load holding valves operated by external pilot pressure , Patent EP 2071195 A2," 2009.

[48] C. Williamson and M. Ivantysynova, "The Effect of Pump Efficiency on Displacement-Controlled Actuator Systems," in *The Tenth Scandinavian International Conference on Fluid Power*, 2007, pp. 301–326.